

Enhanced Polyester Degradation through Transesterification with Salicylates

Hee Joong Kim,[†] Marc A. Hillmyer,^{‡,*} Christopher J. Ellison^{†,*}

[†]Department of Chemical Engineering & Materials Science and [‡]Department of Chemistry, University of Minnesota, Minneapolis, MN, 55455, United States

Keywords: Biodegradable polymers, Polyesters, Transesterification

ABSTRACT: Polyesters constitute nearly 10% of the global plastic market, but most are essentially non-degradable under ambient conditions or in engineered environments. A range of degradable polyesters have been developed as more sustainable alternatives; however, limitations of practical degradability and scalability have hindered their viability. Here we utilized transesterification approaches, including *in-situ* polymerization-transesterification, between a salicylate and a polyester to incorporate salicylate units into commercial polyester backbones. The strategy is scalable and practically relevant given that high molar mass polymers can be obtained from melt-processing of commercial polyesters using common compounders or extruders. Polylactide containing sparse salicylate moieties shows enhanced hydrolytic degradability in aqueous buffer, seawater, and alkaline solutions without sacrificing the thermal, mechanical, and O₂ barrier properties of the parent material. Additionally, salicylate sequences were incorporated into polycaprolactone and a derivative of poly(ethylene terephthalate), and those polymers also exhibited facile degradation behavior in alkaline solution, further expanding the scope of this approach. This work provides insights and direction for the development of high performance yet more sustainable and degradable alternatives to conventional polyesters.

INTRODUCTION

Most commodity polymers are essentially non-degradable and widely found in single-use packaging.¹ Not surprisingly, approximately 56 million metric tons (Mt) of plastic packaging materials ended up in landfills and/or the natural environment in 2016;¹⁻² the accumulated plastic waste in our oceans is projected to reach 900 Mt by 2050.²⁻³ Advances in new recycling and upcycling approaches, including sustainable incineration and chemical/mechanical recycling, are being explored for addressing the growing plastic waste problem.^{1,3} In addition, biodegradable polymers, some of which can be converted into water, carbon dioxide, and biomass under appropriate biologically active conditions after their intended use, represent one possible end-of-life solution.⁴⁻⁷ Polylactide (PLA) is one example, with an estimated global demand on the order of 1 Mt in 2020.⁸ Nevertheless, some polymers labeled as degradable lack facile degradability in natural environments.^{4,9} For example, PLA must be exposed to elevated temperature, high humidity, and appropriate microorganism populations in industrial composting facilities to induce full degradation over reasonable time frames (e.g., months) and is not readily degradable in natural environments.⁴

Among molecular factors that influence polymer degradation, the glass transition temperature (T_g) and molar mass are important characteristics to consider.¹⁰⁻¹² Polyesters are mostly required to be at or above their T_g s to promote their hydrolytic degradation through an increase in chain mobility within the amorphous regions, making high T_g polymers more difficult and energy intensive to degrade.^{8,10} Low T_g polymers, e.g., poly(butylene adipate terephthalate) (PBAT), have been

developed to enhance ambient degradability, however, this feature compromises use in applications that require rigidity at room temperature.¹³⁻¹⁴ Moreover, high molar mass is typically required to achieve desirable mechanical properties, but the associated decrease in end-group concentration and molecular mobility are often commensurate with decreased degradation rate.¹⁰ Designing polymers with facile degradability without sacrificing their performance is a critical challenge in the area of sustainable polymers.

Degradable polymers have been developed for a range of applications and include: poly(hydroxyalkanoates),^{5,15} poly(γ -butyrolactone) (PBL),¹⁶⁻¹⁷ PBL containing trans-ring structures,¹⁸ and polyolefins with silyl-ethers, fused cycles, or ketones.¹⁹⁻²³ Unfortunately, many of these examples are derived from fossil resources,²¹⁻²³ require complicated monomer/polymer/catalyst synthesis steps,^{5,15,18-20,22} show limited (co)polymerization efficiency,¹⁶⁻¹⁷ display limited degradability,^{21,23} and/or would likely experience significant technological hurdles with respect to scalability. We demonstrate a powerful strategy to incorporate readily cleavable salicylate moieties²⁴ directly into polyesters through a straightforward transesterification approach. We posit that this transesterification approach could be cost-efficient and industrially relevant by using commercially available polyesters and practical melt modification techniques in a similar manner to transesterification strategies used to compatibilize polymer blends,²⁵ incorporate new functional units,¹⁷ and produce polymer networks.²⁶ This approach builds on our recent demonstration that salicylic acid, a hydrolysis product from synthesized salicylate-based polymers, can induce autocatalytic acceleration of aq-

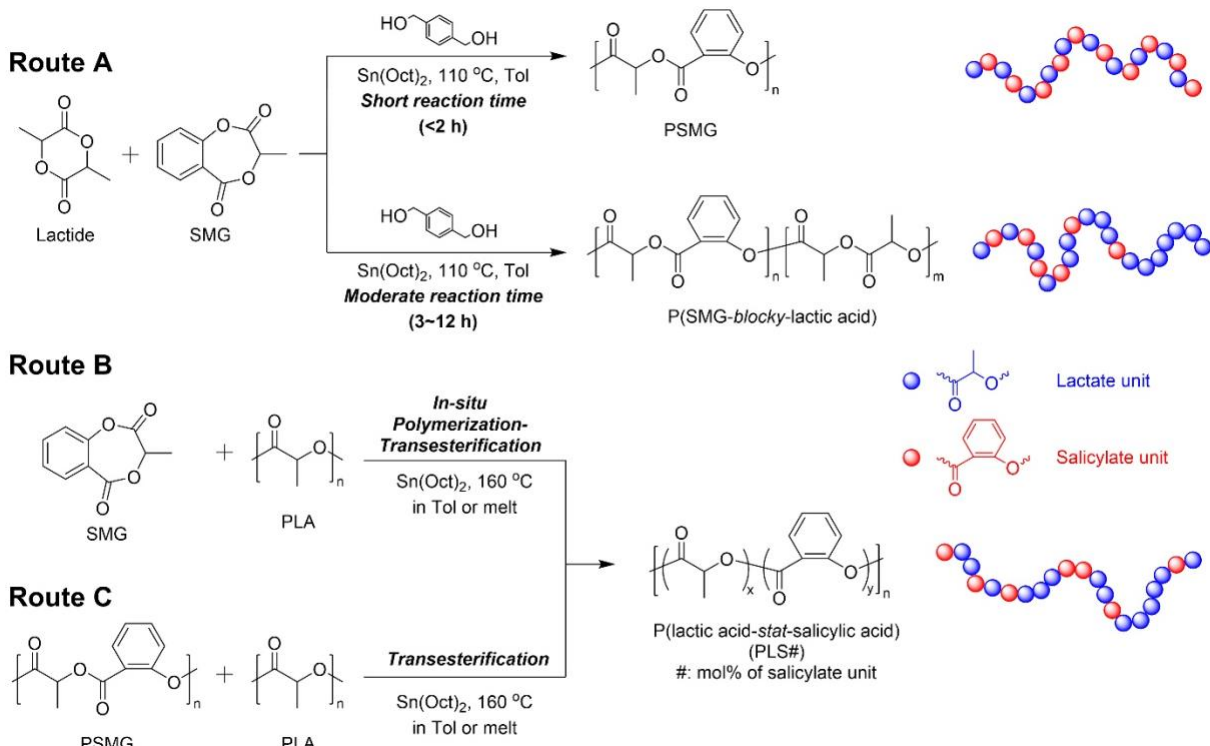


Figure 1. Synthetic pathways to produce PLS.

uous degradation given its relatively high acidity ($pK_a \approx 2.3$).²⁴ Here, we show that by incorporating salicylate units into PLA using melt modification techniques, results in materials with comparable thermal, mechanical, and gas barrier properties to the parent PLA, while also exhibiting enhanced degradability characteristics. We further employ this strategy with commercially relevant poly(caprolactone) (PCL) and poly(ethylene glycol-*co*-cyclohexanediethanol terephthalate) (PETg), considerably expanding the scope of this approach for the development of next generation sustainable polymers.

RESULTS AND DISCUSSION

Ring-opening transesterification copolymerization of lactide and salicylic methyl glycolide (SMG) was carried out in presence of $\text{Sn}(\text{Oct})_2$ (Route A in **Figure 1** and entries 1–4 in Table S1). A reaction time of 2 h at 110 °C resulted in the production of poly(salicylic methyl glycolide) (PSMG) homopolymer with very little lactide incorporation, and a blocky polymer was produced at longer reaction times (3–12 h). The microstructure of the copolymer was investigated by ^1H NMR spectroscopy (**Figure 2a**), and both lactate (L) and salicylate (S) units were resolved to distinguish the L–L–L homosequence, L–L–S/S–L–L heterosequences, and the S–L–S alternating sequence. The S–L–S alternating signals were predominant at early stages. The L–L–L homosequence signals gradually increased over time with little increase in heterosequences, indicating blocky polymer formation. This result was in agreement with ^{13}C NMR spectroscopy (Figures S2–S3), T_g analysis by differential scanning calorimetry (DSC) (**Figure S4**), and molar mass analysis by size exclusive chromatography (SEC) (**Figure S5**).

We attempted direct incorporation of salicylate moieties into the polyester backbone using transesterification at 160 °C (**Figure 1**, Figure S7 for plausible reactions): either *in-situ*

polymerization-transesterification of SMG and PLA (Route B in **Figure 1**, entries 5–10 in Table S1) or intermolecular transesterification between PSMG and PLA (Route C in **Figure 1**, entries 11–15 in Table S1) using solution-based processes initially (toluene as solvent). PLS# indicates the poly(lactic acid-*stat*-salicylic acid) containing # mol% of salicylate moieties. In the ^1H NMR spectra for Route B, the SMG signals disappeared and S–L–S alternating sequences appeared after 1 h (**Figure 2b**). The S–L–S signals then decreased with increasing L–L–S/S–L–L heterosequence signals over time, suggesting that rapid polymerization of SMG occurred early that was then followed by transesterification. ^1H NMR spectra for Route C showed a decrease in S–L–S alternating sequences and increase in L–L–S/S–L–L heterosequences upon reaction, indicating successful sequence exchange (**Figure 2c**). Based on the ^1H NMR data, the degree of randomness (R) was calculated, where $R = 0$ for a block copolymer and $R = 1$ for a completely random architecture.²⁷ The R value increased to ≈ 0.9 through Routes B and C while plateauing at 0.24 in Route A, further suggesting that statistical distributions could be achieved through transesterification Routes B and C. The statistical distributions were further supported by ^{13}C NMR spectroscopy (Figures S2–S3). Diffusion ordered spectroscopy (DOSY) NMR data suggest that the polymer chains are nearly equally populated with the comonomers (Figure S6). The molar mass of the parent PLA ($M_{n,\text{SEC}} = 111 \text{ kg mol}^{-1}$, $D = 1.3$) decreased slightly (Figure S5); for example, the molar mass of PLS25 through Route B and C was 87 and 83 kg mol $^{-1}$, respectively. This likely originates from side reactions involving trace impurities (e.g., water) that result in chain fragmentation during transesterification (Figure S8).^{25,28}

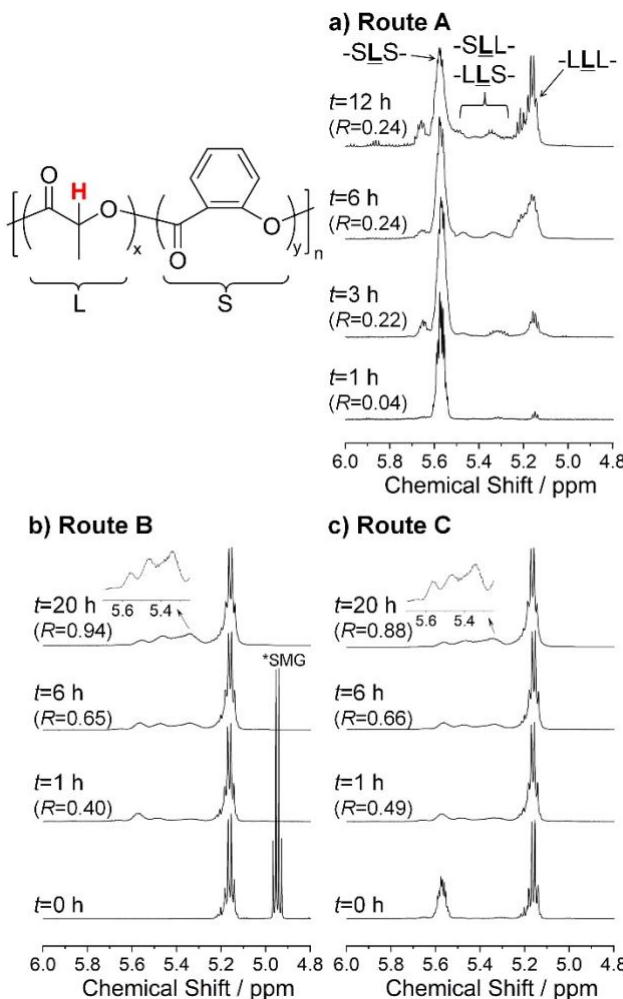


Figure 2. ^1H NMR spectra corresponding to the methine proton region with reaction time for three different synthesis routes of PLS25 (R = degree of randomness).

Both transesterification reactions (Routes B and C) were also carried out in the melt using a twin screw microcompounder ($160\text{ }^\circ\text{C}$, 3 h) using di-*n*-octyltin oxide (DOTO) as a catalyst. Through this bulk and scalable process, PLS with a near-random distribution ($R = 0.79\text{--}0.85$) was obtained with high SMG conversion ($> 99\%$) (Table S1, entries 16–17). Transesterification in the melt state showed comparable extent of reaction to that in solution but at shorter reaction times (3 h), bolstering the potential of this approach in practical scenarios. For example, the *in-situ* melt polymerization-transesterification (Route B) is very similar the industrial melt-processes for grafting maleic anhydride to polyolefins.²⁹ In addition, the reaction temperature for transesterifications ($160\text{ }^\circ\text{C}$) is close to the typical melt processing temperatures for PLA ($160\text{--}200\text{ }^\circ\text{C}$).³⁰ We note that attempts to implement the direct transesterification between salicylic acid and PLA resulted in significant PLA degradation. See Figures S2–S13 more details.

The thermal and mechanical properties of PLS samples were examined by DSC, thermogravimetric analysis (TGA), and tensile testing. Purified PLS samples with high molar mass and high degree of randomness (Route B, entries 7–9 in Table S1) were utilized to evaluate the properties of the pure polymer. PLS7 showed $T_g = 58\text{ }^\circ\text{C}$, comparable to

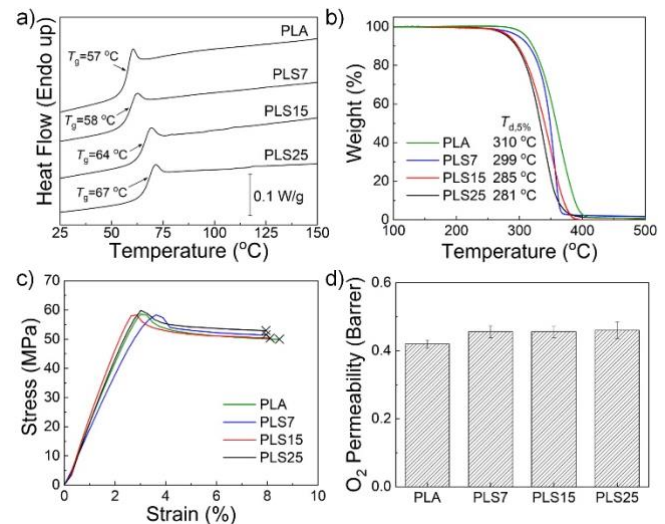


Figure 3. Properties of the synthesized polymers. (a) DSC data (2^{nd} heating, $10\text{ }^\circ\text{C min}^{-1}$), (b) TGA data (under N_2 , $10\text{ }^\circ\text{C min}^{-1}$), (c) representative tensile testing data (ASTM D1708), and (d) O_2 permeabilities.

$T_{\text{g,PLA}} = 57\text{ }^\circ\text{C}$ (Figure 3a). The T_{g} s of PLS increased with increasing salicylate content (e.g., $T_{\text{g,PLS25}} = 67\text{ }^\circ\text{C}$),^{24,31} thus the modifications here slightly increase the T_{g} of the product polyesters as compared to the parent PLA. T_{g} increased in a similar fashion upon the salicylate modification of a semi-crystalline PLLA, and the melting temperature and the degree of crystallinity slightly decreased, presumably due to some disruption of chain packing by the salicylate units (Figure S13d). All PLSs displayed $T_{\text{d,5\%}} \approx 320\text{ }^\circ\text{C}$ ($T_{\text{d,5\%}}$, defined by the temperature of 5% mass loss), comparable to $T_{\text{d,5\%,PLA}} = 338\text{ }^\circ\text{C}$ and other polyesters (e.g., $T_{\text{d,5\%}}$ of poly(γ -methyl caprolactone) $\approx 350\text{ }^\circ\text{C}$, under N_2)³² (Figure 3b, Figure S14 for TGA data in air atmosphere). Isothermal TGA data indicates that purified and crude polymers (i.e., non-purified polymer mixture with $\text{Sn}(\text{Oct})_2$) containing salicylate moieties are stable under typical thermal processing conditions (Figure S15). The PLS displayed a tensile strength of $\sigma_B \approx 58\text{ MPa}$, elastic modulus of $E \approx 2.2\text{ GPa}$, and elongation at break of $\varepsilon_B \approx 7.9\%$ (Figures 3c and S16, Table S2), are all comparable to the parent PLA. In addition, melt-processed crude PLS exhibited comparable mechanical properties to the purified polymers and no significant deterioration in mechanical properties upon reprocessing (Figure S17). To evaluate the potential of these new materials for packaging applications, the oxygen (O_2) permeabilities of the high molar mass PLS samples were also evaluated (Figures 3d and S18). PLA showed O_2 permeability of 0.42 barrer (leak error $\approx 8\%$), comparable to reported values (0.45–0.53 barrer).^{33–34} All PLS samples exhibited comparable O_2 permeability ≈ 0.46 barrer (leak error $\approx 7\%$). In general, PLS displayed comparable thermal, mechanical, and O_2 barrier properties to PLA, demonstrating that statistical incorporation of salicylate sequences into PLA up to 25 mol% does not have a significant impact on these important polymer properties.

Degradation experiments were performed by immersing the copolymers into aqueous solutions, i.e., aqueous phosphate buffer solution (PBS, 1 M, pH 7.4), artificial seawater (pH 8.1), and NaOH solution (0.1 M) (Figures 4a–c). Elevated temperatures ($50\text{ }^\circ\text{C}$) allowed observation of complete degradation over experimentally accessible time frames while remaining below the T_{g} of the samples. Upon

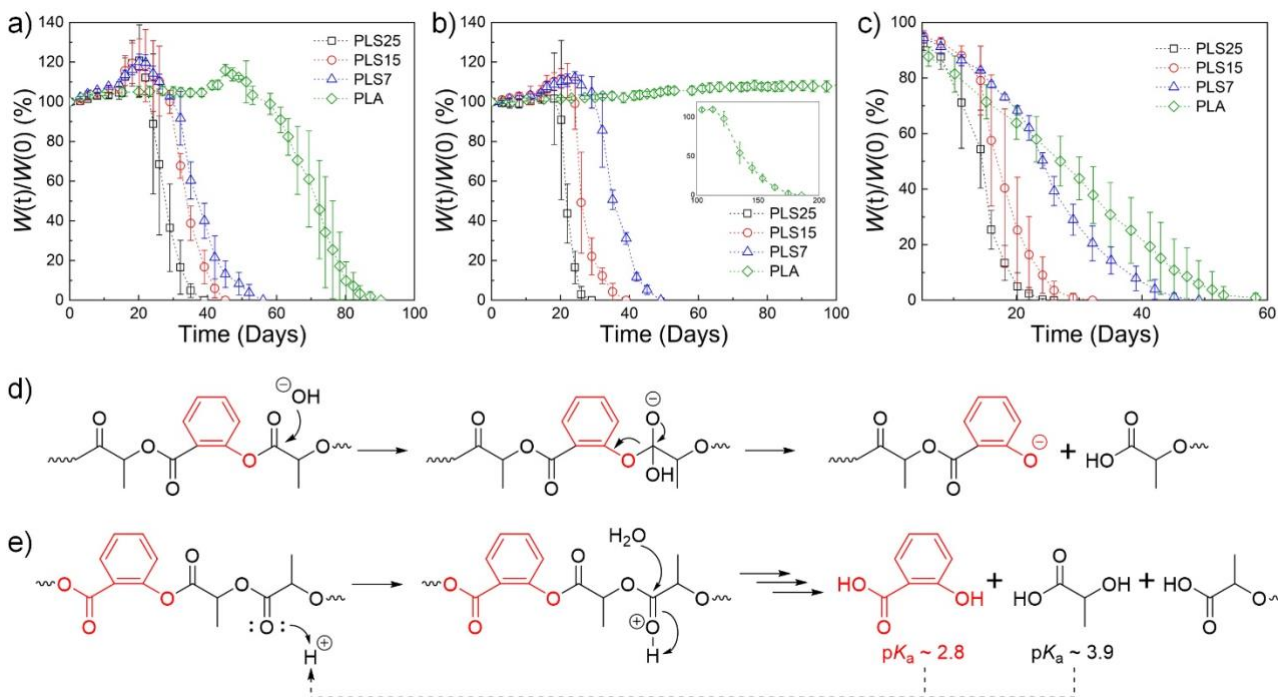


Figure 4. Mass loss profiles of polymers under the hydrolytic degradation conditions at 50 °C in (a) 1 M PBS (pH 7.4), (b) seawater (pH 8.1), and (c) 0.1 M NaOH (*aq.*). Possible facilitated degradation mechanisms of PLS by salicylate sequences under (d) basic and (e) acidic (autocatalysis) conditions.

immersion in PBS, PLS samples showed complete mass loss after a short induction period (**Figure 4a**). We attribute the initial increase in mass during the induction period to water uptake driven in part by osmotic pressure resulting from the bulk erosion process.^{11,35-37} PLA also showed complete mass loss after water uptake, but over a much longer time frame of approximately 90 days, as compared to 40–55 days for the PLS samples, depending on salicylate content.

The accelerative bulk erosive degradation in the PLS samples also occurred in PBS at 40 °C over longer periods, e.g., near complete degradation at 125–150 days (Figure S19). In addition, degradation experiments in PBS were carried out at room temperature (23–27 °C) with exposure to natural sunlight to mimic environmental conditions (Figure S20). Significant mass increases were observed in the PLS15 and PLS25 samples representing the initial stages of water uptake that were followed by rapid degradation at both 40 and 50 °C, but the PLS7 and PLA samples showed only a small mass change (Figure S21). Based on our analysis using the water uptake data at 50, 40, and 23–27 °C and an Arrhenius approach, we estimate that 2.8 years are needed for complete degradation of PLS25 in PBS under ambient conditions (Figure S22).³⁸⁻⁴⁰ This remarkable enhancement is compared to our estimate of full degradation of amorphous PLA under the same condition (5.5 years). However, it is important to note that this time-frame could depend on the shape and thickness of the specific sample undergoing degradation.^{12,36} Photo-oxidative processes represent one possible degradation pathway for polyesters including PBAT and PLA in natural environments,⁴⁰⁻⁴¹ suggesting that the aromatic groups could be beneficial for degradation (Figure S23). PLS displayed even faster bulk erosion in simulated seawater, with complete mass loss of PLS25 over 29 days (**Figure 4b**). In contrast, PLA in seawater showed much slower degradation, likely because of weaker ionic strength conditions in simulated seawater compared to

PBS that drives water uptake and subsequent degradation.^{11,42} Furthermore, PLS showed faster mass loss profiles in an alkaline solution (0.1 M NaOH) than PLA (**Figure 4c**).

We attribute the facile hydrolytic degradation of the PLS samples to the salicylate sequences distributed in the polymer backbone. Readily cleavable salicylate moieties facilitate backbone hydrolysis under basic conditions leading to chain fragmentation (**Figure 4d**). This is consistent with both the short induction periods of PLS samples under near-neutral conditions (**Figures 4a–b** and S19) and faster mass loss profiles of PLS samples as compared to PLA under alkaline conditions (**Figure 4c**). Salicylic acid, one of the hydrolysis products, can also act as a catalyst for chain cleavage during bulk erosion (Figure S24 for hydrolysis products). The salicylic acid pK_a (≈ 2.8)⁴³ is lower than that for lactic acid (≈ 3.9),⁴⁴ which results in faster generation of other acidic hydrolysis products, leading to an amplified degradation cascade (**Figure 4e**).^{24,45} This is consistent with the autocatalytic bulk erosion of PLS samples in PBS and in simulated seawater. PLS2, containing a very small amount of salicylate moieties, showed only slightly faster degradation than PLA, possibly due to the small salicylate content, further confirming the critical role of salicylate moieties for facilitating degradation (Figure S25). Moreover, the hydrolytic degradation rates of PLS samples were comparable to PSMG homopolymer in spite of relatively lower salicylate content.²⁴ This is likely because amorphous PLS ($T_g \approx 58-67$ °C) is somewhat more mobile at the degradation temperatures as compared to the PSMG ($T_g \approx 78-85$ °C), enhancing the degradation process.^{10,12,24,31} Furthermore, two hydrolysis products (i.e., salicylic acid and lactic acid) are essentially benign and have been approved by the FDA for some uses,⁵¹⁻⁵² lessening the concerns over any negative impact of PLS degradation products.

To expand the scope of the strategy described above, salicylate moieties were incorporated into poly(caprolactone)

(PCL) and poly(ethylene glycol-*co*-cyclohexanediethanol terephthalate) (PETg) in solution or melt state. PCL has been widely used commercial polymer, however, its slow degradation limits the range of applications, making it a desirable candidate to explore imparting tunable degradability.⁴⁶⁻⁴⁸ PETg, an amorphous derivative of PET, that also degrades slowly under ambient conditions, was selected because it has been widely used in many applications (e.g., packaging, bottles) and the relative ease with which it can be handled (e.g., soluble in organic solvents, low processing temperature) allows us to readily achieve some extent of transesterification compared to semi-crystalline PET.^{31,49-50} The copolymers were synthesized by *in-situ* solution or melt-state polymerization-transesterification of SMG and each polymer (Route B, Figure S26, and Table S3). ¹H NMR spectra of poly(caprolactone-*stat*-lactic acid-*stat*-salicylic acid) (PCLS) and poly(ethylene glycol-*stat*-terephthalate-*stat*-cyclohexanediethanol-*stat*-lactic acid-*stat*-salicylic acid) (PETCLS) showed that salicylate and lactate were incorporated into the polymer backbone in a similar fashion as compared to PLS ($R_{PCL} = 0.70\text{--}0.78$, $R_{PETCLS} = 0.75\text{--}0.81$, Figures S27–S29). The successful synthesis was further confirmed by SEC (Figures S30–S31) and DSC (Figures S32–S33) analyses.

Degradation experiments were carried out by immersing the polymers into alkaline solution (Figure S35). Given that the parent PCL and PETg hydrolytically degrade quite slowly under ambient conditions, we intentionally used more aggressive degradation conditions (2 M NaOH, 50 °C) to evaluate the degradability over reasonable time frames. PCLS showed enhanced degradation as compared to PCL with complete mass loss over 100 days, demonstrating that salicylate moieties played a critical role in facilitating degradation (Figure S35a). PETCLS displayed continuous mass loss and reached $\approx 45\%$ mass loss over 220 days while PETg showed only a small mass loss ($\approx 10\%$) over 220 days, confirming again that salicylate is a key molecular element for enhancing hydrolytic degradation (Figure S35b). Although the relative degradation of PETCLS is slow compared to the PLA-based samples, inducing significant base degradability into PETg by the incorporation of salicylate sequences could be an important for further chemical recycling processes. The facile degradation of PCLS and PETCLS is likely attributed to chain fragmentation by the cleavage of salicylate linkages, thereby producing low molar mass oligomers that degrade more easily and/or have enhanced permeability to water.¹⁰ See Figures S35–S38 more details.

CONCLUSION

This study demonstrates that salicylate sequences can be incorporated into PLA by established, convenient, practical and effective transesterification approaches. The synthesized PLS samples showed enhanced degradability in all aqueous media without exhibiting a significant trade-off in thermal stability, mechanical properties, or O₂ permeability compared to the parent PLA. In addition, by controlling the salicylate content, the degradation rate was tuned in a controllable manner. Furthermore, the versatility of the transesterification strategy was highlighted by incorporating salicylate sequences into PCL and PETg. The modified PCL and PETg exhibited enhanced degradability, further expanding the scope of this strategy. The materials and approaches described in this study highlight potentially scalable modifications to commercially available polyesters that improve their sustainability through more facile degradation characteristics.

ASSOCIATED CONTENT

Supporting Information. The Supporting Information is available free of charge via the Internet at <http://pubs.acs.org>. Detailed experimental procedures and discussions, monomer conversion data, ¹H, ¹³C NMR, and DOSY NMR data, SEC data, DSC data, TGA data, tensile test results, O₂ permeation data, degradation profiles, estimations for the full-degradation, UV-Vis spectra, and MALDI-TOF data (PDF).

AUTHOR INFORMATION

Corresponding Authors

*Marc A. Hillmyer – Department of Chemistry, University of Minnesota, MN, 55455, United States; ORCID: 0000-0001-8255-3853

e-mail: hillmyer@umn.edu

*Christopher J. Ellison – Department of Chemical Engineering & Materials Science, University of Minnesota, MN, 55455, United States; ORCID: 0000-0002-0393-2941

e-mail: cellison@umn.edu

Author

Hee Joong Kim – Department of Chemical Engineering & Materials Science, University of Minnesota, MN, 55455, United States; ORCID: 0000-0001-6297-1636

e-mail: kim00244@umn.edu

Author Contributions

The manuscript was written through contributions of all authors. All authors have given approval to the final version of the manuscript.

Notes

The authors declare no competing financial interest.

ACKNOWLEDGMENT

We acknowledge our principal funding source, the National Science Foundation Center for Sustainable Polymers at the University of Minnesota, which is a National Science Foundation supported a Center for Chemical Innovation (CHE-1901635). We thank to Yuheng Miao and Youngsu Shin for experimental supports, and Xiayu Peng, Derek Batiste, and C. Maggie Lau for helpful feedback. We also thank to Dr. Chris Derosa for synthesizing PCL, Nicholas Van Zee for helping with DOSY NMR, and Dr. Lucie Fournier for helping with MALDI-TOF analysis.

REFERENCES

- (1) Geyer, R.; Jambeck, J. R.; Law, K. L. Production, use, and fate of all plastics ever made. *Sci Adv*. **2017**, *3* (7), No. 7, e1700782, DOI: 10.1126/sciadv.1700782.
- (2) World Economic Forum, Ellen MacArthur Foundation and McKinsey & Company, The New Plastics Economy: Rethinking the Future of Plastics 2016; www.ellenmacarthurfoundation.org/publications/the-newplastics-economy-rethinking-the-future-of-plastics (accessed 2021-07-03).
- (3) MacArthur, D. E. Beyond plastic waste. *Science* **2017**, *358* (6365), 843-843.
- (4) Haider, T. P.; xVolker, C.; Kramm, J.; Landfester, K.; Wurm, F. R. Plastics of the Future? The Impact of Biodegradable Polymers on the Environment and on Society. *Angew. Chem. Int. Ed.* **2019**, *58* (1), 50-62.
- (5) Tang, X. Y.; Westlie, A. H.; Caporaso, L.; Cavallo, L.; Falivene, L.; Chen, E. Y. X. Biodegradable Polyhydroxyalkanoates by Stereoselective Copolymerization of Racemic Diolides: Stereocontrol

and Polyolefin-Like Properties. *Angew. Chem. Int. Ed.* **2020**, *59* (20), 7881-7890.

(6) Schneiderman, D. K.; Hillmyer, M. A. 50th Anniversary Perspective: There Is a Great Future in Sustainable Polymers. *Macromolecules* **2017**, *50* (10), 3733-3750.

(7) Zimmerman, J. B.; Anastas, P. T.; Erythropel, H. C.; Leitner, W. Designing for a green chemistry future. *Science* **2020**, *367* (6476), 397-400.

(8) Sin, L. T.; Tueen, B. S. *Polylactic acid: a practical guide for the processing, manufacturing, and applications of PLA*. William Andrew, 2019.

(9) Albertsson, A. C.; Hakkarainen, M. Designed to degrade Suitably designed degradable polymers can play a role in reducing plastic waste. *Science* **2017**, *358* (6365), 872-873.

(10) Woodard, L. N.; Grunlan, M. A. Hydrolytic Degradation and Erosion of Polyester Biomaterials. *ACS Macro Lett.* **2018**, *7* (8), 976-982.

(11) Li, S.; Garreau, H.; Vert, M. Structure-property relationships in the case of the degradation of massive poly (α -hydroxy acids) in aqueous media. *J. Mater. Sci.: Mater. Med.* **1990**, *1* (4), 198-206.

(12) Vert, M.; Mauduit, J.; Li, S. M. Biodegradation of PLA/GA Polymers - Increasing Complexity. *Biomaterials* **1994**, *15* (15), 1209-1213.

(13) Mecking, S. Nature or petrochemistry? Biologically degradable materials. *Angew. Chem. Int. Ed.* **2004**, *43* (9), 1078-1085.

(14) Witt, U.; Yamamoto, M.; Seeliger, U.; Müller, R. J.; Warzelhan, V. Biodegradable polymeric materials - not the origin but the chemical structure determines biodegradability. *Angew. Chem. Int. Ed.* **1999**, *38* (10), 1438-1442.

(15) Tang, X. Y.; Westlie, A. H.; Watson, E. M.; Chen, E. Y. X. Stereosequenced crystalline polyhydroxyalkanoates from diastereomeric monomer mixtures. *Science* **2019**, *366* (6466), 754-758.

(16) Hong, M.; Chen, E. Y. X. Completely recyclable biopolymers with linear and cyclic topologies via ring-opening polymerization of γ -butyrolactone. *Nat. Chem.* **2016**, *8* (1), 42-49.

(17) Liu, X.; Hong, M.; Falivene, L.; Cavallo, L.; Chen, E. Y. X. Closed-Loop Polymer Upcycling by Installing Property-Enhancing Comonomer Sequences and Recyclability. *Macromolecules* **2019**, *52* (12), 4570-4578.

(18) Zhu, J. B.; Watson, E. M.; Tang, J.; Chen, E. Y. X. A synthetic polymer system with repeatable chemical recyclability. *Science* **2018**, *360* (6387), 398-403.

(19) Shieh, P.; Nguyen, H. V. T.; Johnson, J. A. Tailored silyl ether monomers enable backbone-degradable polynorbornene-based linear, bottlebrush and star copolymers through ROMP. *Nat. Chem.* **2019**, *11* (12), 1124-1132.

(20) Shieh, P.; Zhang, W. X.; Husted, K. E. L.; Kristufek, S. L.; Xiong, B. Y.; Lundberg, D. J.; Lem, J.; Veysset, D.; Sun, Y. C.; Nelson, K. A.; Plata, D. L.; Johnson, J. A. Cleavable comonomers enable degradable, recyclable thermoset plastics. *Nature* **2020**, *583* (7817), 542-547.

(21) Hsu, T. G.; Zhou, J. F.; Su, H. W.; Schrage, B. R.; Ziegler, C. J.; Wang, J. P. A Polymer with "Locked" Degradability: Superior Backbone Stability and Accessible Degradability Enabled by Mechanophore Installation. *J. Am. Chem. Soc.* **2020**, *142* (5), 2100-2104.

(22) Lin, Y. J.; Kouznetsova, T. B.; Craig, S. L. Mechanically Gated Degradable Polymers. *J. Am. Chem. Soc.* **2020**, *142* (5), 2105-2109.

(23) Morgen, T. O.; Baur, M.; Göttker-Schnetmann, I.; Mecking, S. Photodegradable branched polyethylenes from carbon monoxide copolymerization under benign conditions. *Nat. Commun.* **2020**, *11* (1), 3693, DOI: 10.1038/s41467-020-17542-5.

(24) Kim, H. J.; Reddi, Y.; Cramer, C. J.; Hillmyer, M. A.; Ellison, C. J. Readily Degradable Aromatic Polyesters from Salicylic Acid. *ACS Macro Lett.* **2020**, *9* (1), 96-102.

(25) Zhou, L. Y.; Zhao, G. Y.; Jiang, W. Effects of Catalytic Transesterification and Composition on the Toughness of Poly(lactic acid)/Poly(propylene carbonate) Blends. *Ind. Eng. Chem. Res.* **2016**, *55* (19), 5565-5573.

(26) Self, J. L.; Dolinski, N. D.; Zayas, M. S.; de Alaniz, J. R.; Bates, C. M. Bronsted-Acid-Catalyzed Exchange in Polyester Dynamic Covalent Networks. *ACS Macro Lett.* **2018**, *7* (7), 817-821.

(27) Devaux, J.; Godard, P.; Mercier, J. P. Bisphenol-A polycarbonate-poly(butylene terephthalate) transesterification. I. Theoretical study of the structure and of the degree of randomness in four-component copolycondensates. *J. Polym. Sci.: Polym. Phys. Ed.* **1982**, *20* (10), 1875-1880.

(28) Bankova, M.; Kumar, A.; Impalomeni, G.; Ballistreri, A.; Gross, R. A. Mass-selective lipase-catalyzed poly(ϵ -caprolactone) transesterification reactions. *Macromolecules* **2002**, *35* (18), 6858-6866.

(29) Rakotonirina, M. D.; Baron, M.; Siri, D.; Gaudel-Siri, A.; Quinebeche, S.; Flat, J. J.; Gigmes, D.; Cassagnau, P.; Beyou, E.; Guillaneuf, Y. Acyloxyimide derivatives as efficient promoters of polyolefin C-H functionalization: application in the melt grafting of maleic anhydride onto polyethylene. *Polym. Chem.* **2019**, *10* (31), 4336-4345.

(30) Lim, L. T.; Auras, R.; Rubino, M. Processing technologies for poly(lactic acid). *Prog. Polym. Sci.* **2008**, *33* (8), 820-852.

(31) Kim, H. J.; Peng, X.; Shin, Y.; Hillmyer, M. A.; Ellison, C. J. Blend Miscibility of Poly (ethylene terephthalate) and Aromatic Polyesters from Salicylic Acid. *J. Phys. Chem. B.* **2021**, *125* (1), 450-460.

(32) Batiste, D. C.; Meyersohn, M. S.; Watts, A.; Hillmyer, M. A. Efficient Polymerization of Methyl- ϵ -Caprolactone Mixtures To Access Sustainable Aliphatic Polyesters. *Macromolecules* **2020**, *53* (5), 1795-1808.

(33) Martucci, J. F.; Ruseckaite, R. A. Three-Layer Sheets Based on Gelatin and Poly(lactic acid), Part 1: Preparation and Properties. *J. Appl. Polym. Sci.* **2010**, *118* (5), 3102-3110.

(34) Jain, S.; Reddy, M. M.; Mohanty, A. K.; Misra, M.; Ghosh, A. K. A New Biodegradable Flexible Composite Sheet from Poly(lactic acid)/Poly(ϵ -caprolactone) Blends and Micro-Talc. *Macromol. Mater. Eng.* **2010**, *295* (8), 750-762.

(35) Gorras, G.; Pantani, R. Hydrolysis and Biodegradation of Poly(lactic acid). *Adv. Polym. Sci.* **2018**, *279*, 119-151, DOI: 10.1007/12_2016_12.

(36) Grizzi, I.; Garreau, H.; Li, S.; Vert, M. Hydrolytic Degradation of Devices Based on Poly(DL-Lactic Acid) Size-Dependence. *Biomaterials* **1995**, *16* (4), 305-311.

(37) von Burkersroda, F.; Schedl, L.; Gopferich, A. Why degradable polymers undergo surface erosion or bulk erosion. *Biomaterials* **2002**, *23* (21), 4221-4231.

(38) Han, X. X.; Pan, J. Z.; Buchanan, F.; Weir, N.; Farrar, D. Analysis of degradation data of poly(L-lactide-*co*-L,D-lactide) and poly(L-lactide) obtained at elevated and physiological temperatures using mathematical models. *Acta Biomater.* **2010**, *6* (10), 3882-3889.

(39) Codari, F.; Lazzari, S.; Soos, M.; Storti, G.; Morbidelli, M.; Moscatelli, D. Kinetics of the hydrolytic degradation of poly(lactic acid). *Polym. Degrad. Stab.* **2012**, *97* (11), 2460-2466.

(40) Chamas, A.; Moon, H.; Zheng, J. J.; Qiu, Y.; Tabassum, T.; Jang, J. H.; Abu-Omar, M.; Scott, S. L.; Suh, S. Degradation Rates of Plastics in the Environment. *ACS Sustain. Chem. Eng.* **2020**, *8* (9), 3494-3511.

(41) De Ho, G. X.; Zumstein, M. T.; Getzinger, G. J.; Ruegsegger, I.; Kohler, H. P. E.; Maurer-Jones, M. A.; Sander, M.; Hillmyer, M. A.; McNeill, K. Photochemical Transformation of Poly(butylene adipate-*co*-terephthalate) and Its Effects on Enzymatic Hydrolyzability. *Environ. Sci. Technol.* **2019**, *53* (5), 2472-2481.

(42) Li, S. M.; Garreau, H.; Vert, M. Structure-property relationships in the case of the degradation of massive aliphatic poly(α -hydroxy acids) in aqueous media. *J. Mater. Sci.: Mater. Med.* **1990**, *1* (3), 123-130.

(43) Volgyi, G.; Ruiz, R.; Box, K.; Comer, J.; Bosch, E.; Takacs-Novak, K. Potentiometric and spectrophotometric pK_a determination of water-insoluble compounds: Validation study in a new cosolvent system. *Anal. Chim. Acta* **2007**, *583* (2), 418-428.

(44) Haynes, W. M. *CRC handbook of chemistry and physics*. CRC press, 2014.

(45) Miller, K. A.; Morado, E. G.; Samanta, S. R.; Walker, B. A.; Nelson, A. Z.; Sen, S.; Tran, D. T.; Whitaker, D. J.; Ewoldt, R. H.; Braun, P. V.; Zimmerman, S. C. Acid-Triggered, Acid-Generating, and Self-Amplifying Degradable Polymers. *J. Am. Chem. Soc.* **2019**, *141* (7), 2838-2842.

(46) Dankers, P. Y. W.; Harmsen, M. C.; Brouwer, L. A.; Van Luyn, M. J. A.; Meijer, E. W. A modular and supramolecular approach to bioactive scaffolds for tissue engineering. *Nat. Mater.* **2005**, *4* (7), 568-574.

(47) Bartnikowski, M.; Dargaville, T. R.; Ivanovski, S.; Hutmacher, D. W. Degradation mechanisms of polycaprolactone in the context of chemistry, geometry and environment. *Prog. Polym. Sci.* **2019**, *96*, 1-20.

(48) Hakkarainen, M.; Höglund, A.; Odelius, K.; Albertsson, A.-C. Tuning the Release Rate of Acidic Degradation Products through Macromolecular Design of Caprolactone-Based Copolymers. *J. Am. Chem. Soc.* **2007**, *129* (19), 6308-6312.

(49) Kibler, C. J.; Bell, A.; Smith, J. G. Polyesters of 1,4-cyclohexanedimethanol. *J. Polym. Sci. Part A: General Papers* **1964**, *2* (5), 2115-2125.

(50) Turner, S. R. Development of amorphous copolymers based on 1,4-cyclohexanedimethanol. *J. Polym. Sci. Polym. Chem.* **2004**, *42* (23), 5847-5852.

(51) U.S. Department of Health & Human Services, Food and Drug Administration (FDA). Code of Federal Regulations, Section 184.1061. *Food and drugs: Part 184-direct food substances affirmed as generally recognized as safe*, last revised April 2020. <https://www.accessdata.fda.gov/scripts/cdrh/cfdocs/cfcfr/cfrsearch.cfm?fr=184.1061> (accessed 08-23-2021).

(52) U.S. Department of Health & Human Services, Food and Drug Administration (FDA). Code of Federal Regulations, Section 333.310. *Food and drugs: Part 333-topical antimicrobial drug products for over-the-counter human use*, last revised April 2020. <https://www.accessdata.fda.gov/scripts/cdrh/cfdocs/cfcfr/CFRSearch.cfm?CFRPart=333&showFR=1&subpartNode=21:5.0.1.1.14.4> (accessed 08-23-2021).

Table of Contents artwork

